

Temperature dependence of magnetic resonance probes for use as embedded sensors in constructed wetlands

Theodore Hughes-Riley*, Elizabeth R. Dye, Dario Ortega Anderrez, Fraser Hill-Casey†, Michael I. Newton and Robert H. Morris

School of Science and Technology, Nottingham Trent University, United Kingdom.

† Mr Hill-Casey is now at Sir Peter Mansfield Imaging Centre, School of Medicine, University of Nottingham, Nottingham, NG7 2RD, United Kingdom

* Author to whom correspondence should be addressed;
E-Mail: hughesriley@gmail.com;
Tel.: +44 (0) 115 848 3315

Highlights

- Magnetic resonance sensors work over an environmentally relevant range of temperatures.
- Signal losses at the temperature range extremities are characterized and explained.
- Data is recorded in an operational wetland over 203 days.

Abstract

Constructed wetlands are now accepted as an environmentally friendly means of wastewater treatment however, their effectiveness can be limited by excessive clogging of the pores within the gravel matrix, making this an important parameter to monitor. It has previously been shown that the clog state can be characterised using magnetic resonance (MR) relaxation parameters with permanent magnet based sensors. One challenge with taking MR measurements over a time scale on the order of years is that seasonal temperature fluctuations will alter both the way that the sensor operates as well as the relaxation times recorded. Without an understanding of how the sensor will behave under different temperature conditions, meaningful information about the clog state cannot be successfully extracted from a wetland. This work reports the effect of temperature on a permanent magnet based MR sensor to determine if the received signal intensity is significantly compromised as a result of large temperature changes, and whether meaningful relaxation data can be extracted over the temperature range of interest. To do this, the central magnetic field of the sensor was monitored as a function of temperature, showing an expected linear relationship. Signal intensity was measured over a range of temperatures (5 °C to 44 °C) for which deterioration at high and low temperatures compared to room temperature was observed. The sensor was still operable at the extremes of this range and the reason for the signal loss has been studied and explained. Spin-lattice relaxation time measurements using the sensor at different temperatures have also been taken on a water sample and seem to agree with literature values. Further to this, measurements have been taken in an operational

Published article DOI: [10.1016/j.sna.2016.01.050](https://doi.org/10.1016/j.sna.2016.01.050)

© 2016. This manuscript version is made available under the CC-BY-NC-ND 4.0 license

<http://creativecommons.org/licenses/by-nc-nd/4.0/>

wetland over the course of 203 days and have shown a linear dependence with temperature as would be expected. This work concluded that the sensor can perform the task of measuring the spin-lattice relaxation time over the required temperature range making it suitable for long-term application in constructed wetlands.

Keywords: constructed wetlands; time domain magnetic resonance; clog state; spin-lattice relaxation; embedded sensor; temperature dependence

1. Introduction

Constructed wetland (CW) technology began to proliferate heavily in Europe during the 1980's and 90's, as well as in North America, and now is a commonly employed method for water treatment in both regions, as well as in China where the CW has gained increasing interest since the late 1990's [1], [2]. A CW comprises of an aggregate matrix, typically gravel, through which the wastewater is mechanically filtered and where microorganisms grow. Over time a build-up of particulate and excessive biofilm growth occludes the pores preventing successful transfer of the wastewater through the bed. Eventually a critical point is reached where the bed can no longer treat wastewater and floods, typically after a decade [3]. Reconditioning of a wetland after it has become critically clogged is a time consuming and expensive process, and should therefore be avoided if possible. As a result, it is important to monitor the clogging level of systems to allow for optimal treatment efficiency. Ascertaining the clog state is also a useful research tool when examining wetland operation and design.

A number of methods exist to characterize the clog state in the literature and these fall into three general categories, the measurement of hydraulic conductivity [4], determining the hydrodynamics of the system on a larger scale using tracer dyes (such as Rhodamine WT) [5], [6], or by determining the quantity of solids present within the pores by drying out a wetland sample [7]. Each of these techniques have their own strengths and weaknesses, and this has been well covered by others [8]. One limitation for all of these methods is that they cannot be automated and require human input either in extracting a sample and analyzing it in a laboratory, or running experiments on site. This ultimately makes taking the measurements costly over the lifetime of a wetland or research study when labor is considered.

An alternative to these methods is by using pulsed (time domain) magnetic resonance (MR) sensors. MR works by a careful manipulation of the magnetic moments of certain nuclei, including the hydrogen in water molecules, using radio frequency (RF) pulses. These typically determine parameters called relaxation times, T_1 , or spin-lattice relaxation and T_2 , or spin-spin relaxation; although another parameter T_2^{eff} is more commonly measured than T_2 with this type of sensor owing to the inherent field inhomogeneity. Sensors like this have found a disparate range of applications in recent years partly due to the reducing cost of micro-electronics [9].

Determining the clog state of both model systems and wetland samples have been extensively investigated in the laboratory setting using relaxation measurements [10], [11], [12], [13], [14]. The parameter T_2^{eff} has been previously used to successfully characterize clogging in a model system where a highly homogeneous magnetic field has been used for MR measurements [11], [12], however this was not possible with the inhomogeneous magnetic field of a low-cost permanent magnet system such as the type used in this work [14]. Therefore this work focusses on T_1 relaxation measurements which have also been used to determine the clog state with a similar sensor in the past [10], [13], [14].

Further investigation has seen a series of MR sensors constructed and permanently embedded into the gravel matrix of a constructed wetland for long term monitoring of the clog state, proving that the sensors can successfully operate in a functioning wetland. To validate their operation over these time scales, selected probes have been extracted and re-tested on known samples in the laboratory environment after a number of months: The only observed change to the sensors was discoloration of the plastic housing of the probes. Fig. 1 shows some example data taken from two probes embedded in mature, operational wetlands (operated by ARM Ltd., Rugeley, UK).

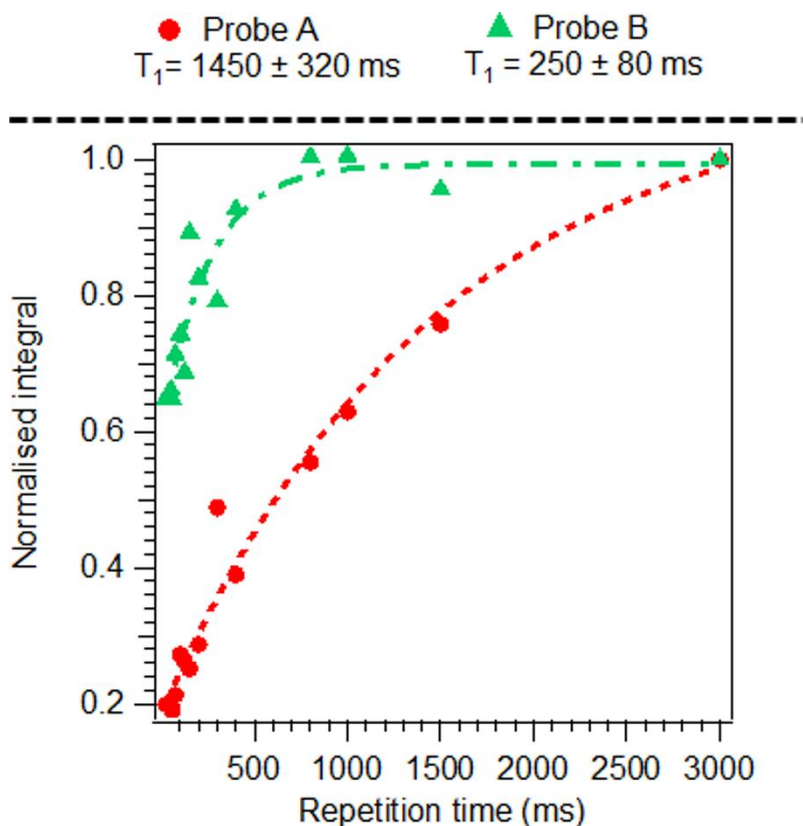


Fig. 1. Example T_1 relaxation data taken from two probes embedded in established constructed wetlands.

Probe A represents a probe in a well-established operational bed, while probe B was in a different bed in a location where significant clogging was believed to be present. There is a factor of ~6 difference between these two values showing a great sensitivity to clog state. This difference would be greater when investigating a newly commissioned bed compared to one that was critically clogged, which would represent the extreme ends of potential clogging scenarios. While useful to validate the technique, there are additional considerations when monitoring an operational wetland over long time scales.

An important consideration is temperature. While a constructed wetland's water temperature is not necessarily the same as the air local temperature [15], seasonal variation will mean that a constructed wetland will be subject to a range of temperatures which depends on location. In order to better validate the sensor technology, the effect of temperature on the operation of the physical sensor and how temperature may affect the sample explored must therefore be understood.

MR measurements are sensitive to the temperature of the sample under test. Temperature is known to heavily affect spin-lattice (T_1) relaxation times in water [16], [17], [18] with a strong linear relationship between the T_1 times and temperature observed between the boiling and freezing points of water. This holds true for the range of temperatures that would typically be encountered by a device left outside (-5 °C to 40 °C) although it should be noted that it is not possible to obtain a signal from water below freezing. This relationship is well understood and has led to the development of MR thermometry [19], [20], [21].

Within an unclogged wetland, the majority of the bed will be free water and aggregate. In the case of a typical aggregate such as gravel only the free water would be detectable by the MR probe, hence T_1 values recorded in an unclogged wetland would be expected to vary with temperature in the same way that it does for water. Clogging occurs within the wetland due to a build-up of sediment and the growth of biofilms, both of which are useful to the treatment of water in the correct quantity. In a clogged wetland these other components representing water with high concentrations of particulate in it, or water comprising biofilms would be detectable by the MR probe [13]. The relaxation times of these components (i.e. particulate associated water and water in biofilm) might not be affected by temperature in the same way as water, however these components are known to have shorter relaxation times than water, so the influence on a final T_1 relaxation time would likely be less significant than the effect of free water. Additionally the root and rhizome network of the aquatic plants growing within the wetland would also be measureable by the MR sensor, however there should be no other materials or pollutants within normal domestic wastewater that would significantly alter the recorded T_1 value. This is not necessarily the case for all wastewater types such as those containing large quantities of hydrocarbons although these are not considered in this work.

The physical effects that temperature has on the sensor must also be considered, as temperature changes are known to effect the magnetic field strength of permanent magnets [22]. In this work we use a 'Helmholtz-style' sensor (shown in Fig. 2) and sensors of a similar design to this have been presented elsewhere [10]. A probe of a comparable design was used to collect a set of preliminary measurements exploring the temperature effects [23] however the design and construction technique has been refined since then. This design used two NbFeB magnets to generate a field in the magnet gap where a six-turn solenoid was placed for the transmission and reception of RF signals. Steel disks were used on each magnet to reduce the magnetic field inhomogeneity however, the magnetic field gradient was still very large. This made the collection of a free induction decay (FID) impossible and rendered many magnetic resonance techniques ineffectual. As a result, signal must always be obtained by collecting an echo [24].

With regards to the constituent magnets of the sensors, a variety of widely available magnet types were considered including ceramic, samarium-cobalt (SmCo) or neodymium-iron-boron magnets (NdFeB). The literature shows that both SmCo and NdFeB have similar properties, producing comparable field strengths and having a similar degree of resistance to a reduction in field due to the application of an external magnetic field [25]. Two major advantages exist for SmCo magnets over NdFeB in that they do not lose their permanent magnetic properties until they reach a comparatively high temperature (800 °C for SmCo compared to 310 °C for NdFeB) [25] and that their magnetic field strength is fairly resilient to changes in temperature, a factor of 3.5 less than for NdFeB magnets. While the resistance of the magnetic field to temperature makes this type of magnet favorable for use outside, where it will experience significant seasonal temperature variations, the typically greater cost of SmCo magnets and their fragility are both poor qualities for an embedded sensor. Additionally, SmCo magnets of a size desirable for these MR sensors were difficult to source off-the-shelf. As a result, NdFeB magnets were initially used for these sensor.

Small increases in the temperature of a NdFeB magnet cause reversible losses in the nuclear magnetisation. Literature dealing with reversible flux losses in NdFeB magnets show small changes at low temperatures [22] compared to the overall magnetic field strength.

The magnetic resonance probes require a tuned radio frequency circuit to be created using the sensor RF coil. This must be tuned and matched to the equivalent magnetic field as determined by the Larmor frequency [26]. The frequency transmitted by the RF coil is sometimes known as the excitation frequency, and where the excitation frequency and Larmor frequencies are the same or very close the on-resonance condition is said to have been achieved. In these cases the greatest signal intensity is often produced. When this is not the case off-resonance excitation is said to have occurred, which can be detrimental to the collected signal intensity in some cases.

Even small changes in the magnetic field strength (as low as 0.015 T) may shift the Larmor frequency outside of the range that the RF coil is capable of transmitting and receiving signals (the bandwidth of the RF coil). It is also possible that due to the magnetic field gradient present between the magnets, that regions may move into and out of the detectable range of the RF coil depending on the temperature of the magnets.

In this work the suitability of a 'Helmholtz style' permanent magnet MR sensor over a range of temperatures was examined to ensure the long term viability of an embedded sensor. The suitability was evaluated at different temperatures to see if the shift in the field intensity of the NdFeB magnets had a significantly detrimental effect on the MR signal strength. This was then extended to a study of different operating Larmor frequencies at three temperatures of interest. T_1 values for water were then recorded with the sensor over a range of temperatures to validate its use at acquiring meaningful relaxation data.

Further to this, measurements were taken in an operational wetland over the course of around 200 days, and the shift in collected T_1 values with respect to temperature changes have been assessed. Ultimately this work determined the viability of these sensors under the conditions they will encounter over their lifetime *in situ*.

2. Experimental Section

2.1. MR sensor design

This study was conducted using sensors in a Helmholtz style configuration, very similar to a design previously presented [10]. Two N42 neodymium magnets (height = 20.0 mm, radius = 17.5 mm; HKCM GmbH, Germany) were arranged with parallel magnetisation and spaced by 20 mm, generating a magnetic field in the magnet aperture (center field strength = 0.2468 T at 292 K), as shown in Fig. 2. Steel disks were used on the faces of the magnets to improve field uniformity (2.0 mm thick; St. Anns Sheet Metal, Nottingham, UK; note that the magnet spacing given is from the top of the steel disk, not the top of the actual magnet).

The magnetic field gradients were recorded within the coil region in three dimensions at room temperature (22 ± 1 °C) using a gaussmeter (Coliy handheld gaussmeter model G93; Coliy Technology GmbH, Duesseldorf, Germany). Measurements were taken from the center of the coil to the extreme edge of the coil in each direction finding that $G_x = 0.29 \pm 0.03$ Tm⁻¹, $G_y = 0.15 \pm 0.06$ Tm⁻¹, $G_z = 0.46 \pm 0.06$ Tm⁻¹. As an FID could not be collected using this experimental set-up, it was not possible to determine the gradient strengths by analyzing the

spectrum. At this temperature the magnetic field strength at the center of the coil region was 0.2468 T, corresponding to a resonant frequency of 10.5 MHz.

The RF transmit-receive coil took the shape of a six-turn solenoid (i.d. = 12 mm, length = 14 mm) made from enameled copper wire (o.d. = 0.5 mm; Rowan Cable Products Ltd., Potters Bar, UK) attached to parallel-series tuning boards with two variable capacitors (5.5 - 50 pF; Johanson Manufacturing, NJ, USA) and a 2.5 m inductive tuning element (BNC cable) completing a resonant circuit capable of operating between 10.2 – 11.5 MHz depending on the values that the variable capacitors were set to. A network analyser (E5061A ENA Series Network Analyser; Agilent Technologies, Santa Clara, USA) was used to find the bandwidth of the coil (full width at -3 dB), which was determined to be 0.5 MHz. The spectrometer receiver bandwidth was set to 1.0 MHz.

The system was initially tuned and matched before each experiment and was subsequently re-tuned as needed throughout this study. The pulse length used was calibrated for each frequency explored, ranging from between 3.8 and 8.1 μs for a 90° pulse. The RF pulse amplitude was doubled for a 180° pulse. The optimal pulse length was not observed to alter with changes in temperature. The different pulse lengths used gave a range of transmission bandwidths from 0.2 MHz up to 0.5 MHz.

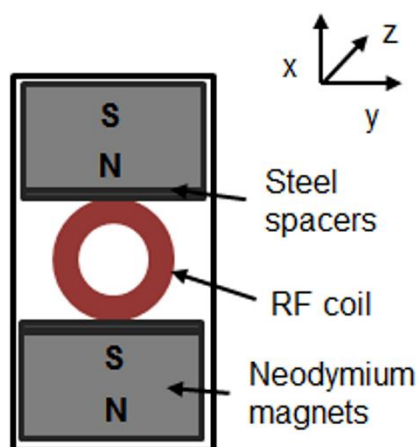


Fig. 2. Schematic representation of the sensor design used in this work. Figure is not to scale.

A second sensor of the same design was used for the wetland study. This probe operated at 11.4 MHz, with an optimal pulse length of 6.8 μs .

2.2. MR measurement protocol

Magnetic resonance experiments were performed using a commercial Kea² spectrometer (Magritek, Wellington, New Zealand) running Prospa 3.22 software. The only MR sequence used in this work was a Carr Purcell Meiboom Gill (CPMG) sequence [27]. For signal intensity measurements, 64 echoes were summed to reduce the number of averages required and an integral over the echo sum was taken to determine an amplitude ($T_E = 150 \mu\text{s}$). A repetition time of 15 s was used to ensure the system fully returned to equilibrium before the next experiment. T_1 measurements were taken using a variable repetition time method (uneven intervals between 25 ms and 15 000 ms) as performed in previous work [10], [13], [14]. When taking readings at the wetland 128 echoes were summed to provide a greater signal intensity.

Laboratory MR experiments were performed with the MR probe submerged in tap water. For the experiments presented, MR measurements saw the probe, sample, and associated electronics located within a copper shielded box to reduce RF noise from the surrounding laboratory environment, where 16 scans were used for all measurements with the exception of the data collected in the wetland, where a copper box could not be utilized necessitating 128 scans. Typically only 32 scans were needed to acquire good relaxation data in the laboratory from the probes when not using the shielding box. Fittings were performed with IGOR Pro (Version 6.3.4.1; Wavemetrics, OR, USA) which was also used to produce the figures.

2.3. Inducing temperature changes

In this study the probe and sample were brought to a given temperature using four methods depending on the desired temperature: a domestic refrigerator, leaving the probe outdoors, leaving the probe indoors, and using a convection oven (FED 53, Binder GmbH, Tuttlingen, Germany) set to two different temperatures (typically 40 °C or 50 °C). The probe and sample would be held at temperature for at least one hour prior to the commencement of MR experiments to ensure a state of thermal equilibrium. The temperature was measured using a type-K thermocouple attached to an electronic thermometer (either from Comark Instruments, Norwich, UK or Omegaette, Karvina, Czech Republic).

For the data shown in Fig. 3, the magnet assembly was first heated using the convection oven and left to cool naturally as required to reach the desired temperature by equilibrating with room temperature (typically around 22 °C). The magnet assembly was then cooled using the refrigerator and left to heat up to room temperature.

For data collected in a wetland, temperature changes were due to actual seasonal variation, and therefore the probe would have normally been held at temperature for many hours beforehand. The wetland used was a mature vertical-flow system located at the main ARM facility (ARM Ltd, Rugeley, UK) which is constructed with gravel with an average diameter of 10 mm.

Errors in the temperature were taken using the standard error of the temperature variations observed over the course of a given set of experiments (temperature measurements were always taken at least four times).

3. Results and Discussion

3.1. Magnetic field strength as a function of temperature

The magnetic field strength at the center of the sensors detection region was investigated as a function of temperature between 2.5 °C and 44.5 °C using the gaussmeter discussed previously (accurate to ± 0.005 mT). While MR can be a powerful tool to determine the field strength of a magnet, the large field gradient produced by the magnet arrangement made an MR based determination of the field strength unnecessarily challenging.

Throughout the experiments described later, it was observed that the tuning and matching electronics remained unaffected by temperature changes in this regime.

It should be noted that the the probe required moving between taking results when the probe was heated, and taking them when the probe was cooled. The gaussmeter was carefully

realigned to the same geometrical point with the magnet gap using a bespoke ABS holder, allowing for repositioning with a high degree of accuracy (within 1 mm in each dimension).

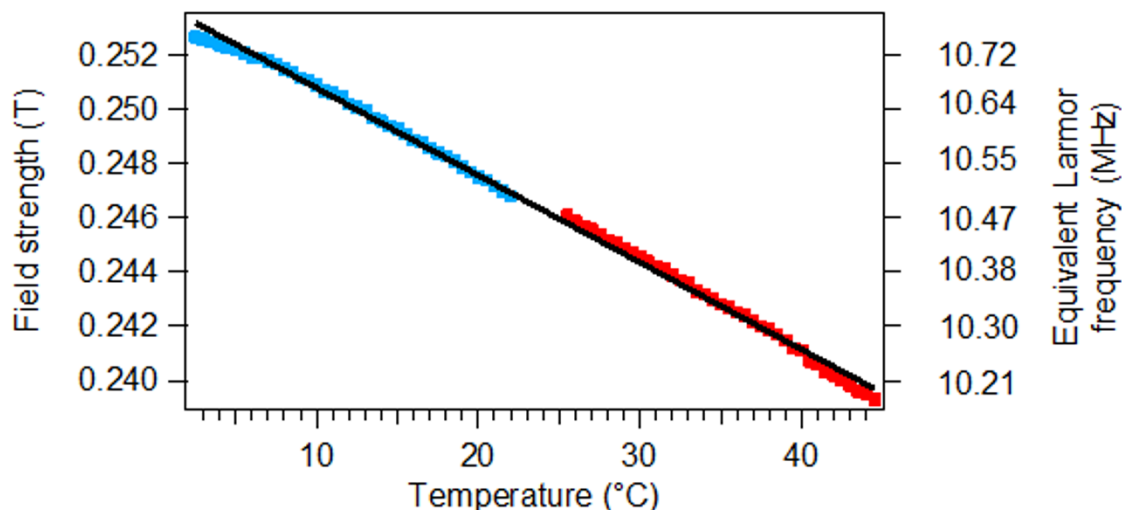


Figure 3. Magnetic field strength in Tesla as a function of temperature. The Larmor frequency of protons is shown on the right. For measurements above 25.5 °C the magnet was heated and left to cool, while for temperatures below 22.0 °C the magnet was cooled and then left to warm.

Fig. 3 showed a close to linear relationship, in keeping with the theory, with the linearity breaking down slightly at the extremes of the temperature range explored. The relationship showed a change of 0.0003 T/°C.

3.2. Magnetic resonance response as a function of temperature

When the magnetic field gradients of the magnet assembly and the range of frequencies that the RF coil could transmit and receive signal at were considered, it was apparent that at no time would the entire volume of the solenoid be detectable through MR measurements. Therefore, assuming that the resonant circuit was tuned roughly to the center frequency of the magnets at the center of the coil at room temperature, then the volume being detected by the coil would decrease at comparatively high and low temperatures. A short study was conducted investigating the signal intensity as a function of temperature at a fixed frequency. Ultimately 10.7 MHz was chosen as a rough frequency calibration showed that this frequency provided the greatest signal intensity at room temperature (as opposed to the center frequency of 10.5 MHz); the results are shown in Fig. 4.

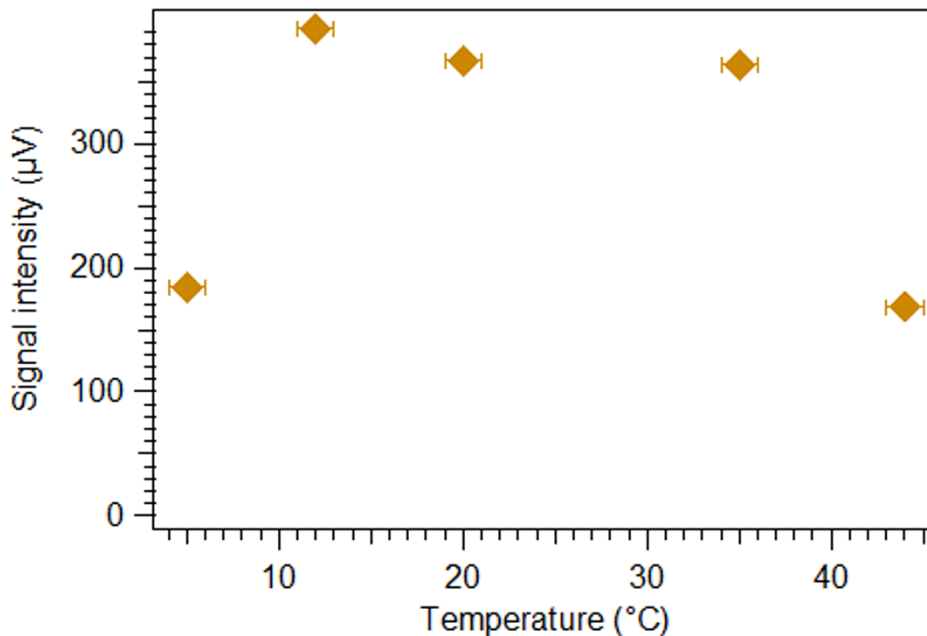


Figure 4. Signal intensity as a function of temperature on a water sample. Each point shown was the average of four measurements with the standard error used to generate error bars.

It was seen that signal intensity at relatively high and low temperatures resulted in a signal reduction of roughly a factor of two and a half compared to the fairly stable region around 20 °C. The optimal signal intensity was due to the overlap between the volume within the magnet gap where the magnetic field strength corresponded to the excitation frequency used to drive the RF coil. Signal would only be collected from nuclei where these conditions were satisfied within the excitation range allowed by the probes transmission bandwidth (0.3 MHz for a 6.1 μ s pulse). A drop-off in the signal would then occur at both high and low temperatures where the Larmor frequency, due to the magnetic field strength, would not correlate well with the range of excited frequencies.

As evident in Fig. 3, the Larmor frequency at the center of the magnet changed with temperature. Optimal operating conditions should have been achieved when the magnetic field near the center of the solenoid was close to the RF coils resonant frequency, however this was not strictly true due to the size of the gradients in the magnet gap (discussed in the MR sensor design section). It was already observed that an excitation frequency of 10.7 MHz provided a superior signal intensity at room temperature than when the actual frequency at the center of the coil, 10.5 MHz was used. This made sense based on the geometry of the field gradient, as the center of the coil was the point furthest away from either magnet, leading to most of the volume inside of the solenoid experiencing a higher magnetic field than at the center.

One cause for signal loss in a system such as this (where there was a large static magnetic field gradient) would be contributions due to off-resonance excitation. Here, multiple coherence pathways could contribute to each overall echo amplitude. These effects have been investigated thoroughly in the literature [28] partly due to their importance for well-logging applications [29]. In a sample where the diffusion in the stray field gradient was non-negligible, contributions from the coherence pathways that are off-resonance would decay rapidly compared to the on-resonance contributions [28]. As the on-resonance regions within the RF coil moved with temperature changes, the contribution from off-resonance coherence

pathways would increase. The more rapid decay of these pathways would therefore lead to a smaller overall signal intensity in these cases.

With the aim of better understanding the observed relationship as well as how the probe would be operated at high and low temperatures, a range of excitation frequencies were explored at different temperatures to see if changing the excitation frequency significantly altered the signal intensity. In this experiment three temperatures were explored (2 ± 0 °C, 18 ± 1 °C, or 46 ± 1 °C). The probe was intentionally tuned off-resonance and a signal intensity was collected (using a pulse length correctly calibrated for that frequency). The frequency was then incrementally increased with a signal intensity taken at each frequency. It was expected that eventually the optimal resonant frequency would be reached, providing the highest signal, followed by the probe being detuned from frequency again.

Ultimately the range 10.2 MHz - 11.5 MHz was explored at three different temperatures. The raw results are shown in Fig. 5(a). The matching of the resonant circuit, which is a factor that affects the overall collected signal intensity, was recorded for each experiment and found to be on average higher for the room temperature measurements (-8.78 ± 0.33 dB for 2 °C, -12.26 ± 0.55 dB for 18 °C, -9.51 ± 0.37 dB for 46 °C). The results after this correction are shown in Fig. S1. Additionally the bandwidth of the probe changed along with the pulse length depending on the frequency used. It was seen that the transmit bandwidth of the probe increased with frequency (shown in Fig. S2). This meant that with a greater bandwidth a larger volume within the coil to be excited. This led to a higher signal intensity. Both of these effects have been compensated for, with the results shown in Fig. 5(b).

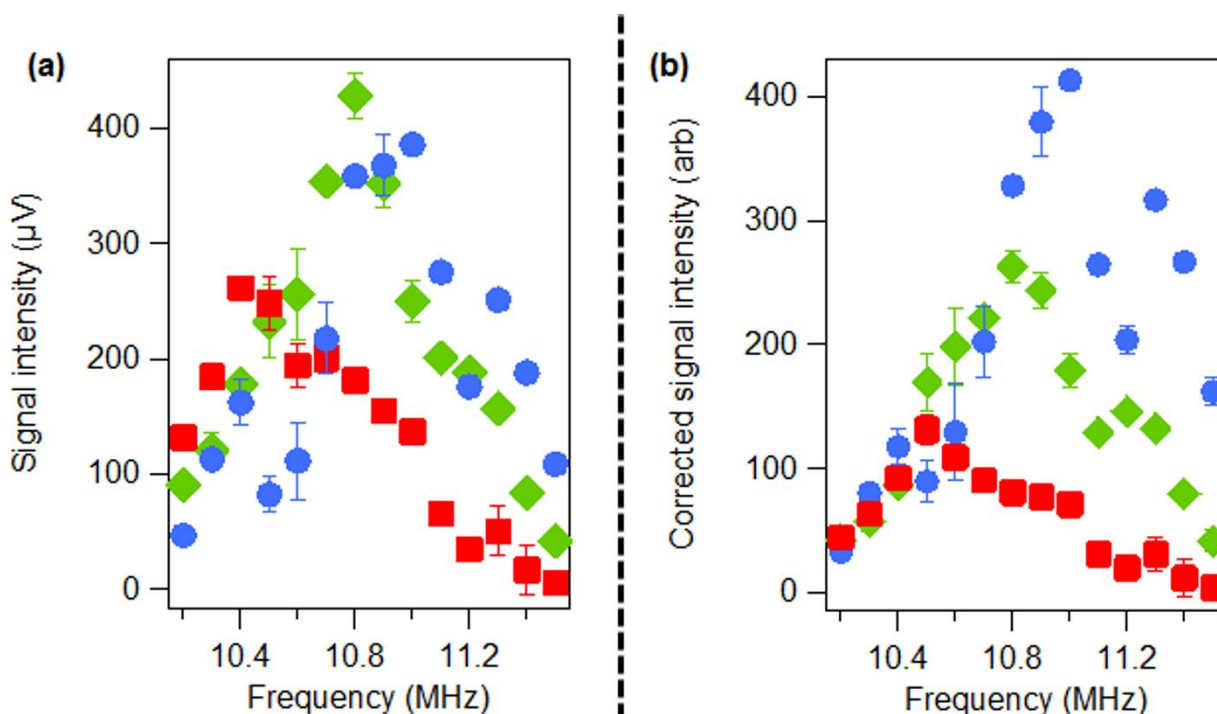


Fig. 5. Signal intensity as a function of frequency on a water sample with the sensor and sample held at three different temperatures: ● 2 ± 0 °C, ◆ 18 ± 1 °C, ■ 46 ± 1 °C. (a) Raw collected signal intensities (b) The collected signal intensity has been corrected to account for the discrepancy in the resonant circuits matching as well as for the bandwidth of the transmitted pulse at different frequencies.

It can be observed (from Fig. 5(a)) that at higher and lower temperatures the signal intensity was less than at room temperature, as seen earlier in Fig. 4. This was also true for when the probe was tuned to its optimal frequency at a given temperature, however it appeared that when colder an overall higher signal intensity could be achieved compared to when warmer. When the inconsistencies with the matching of the resonant circuit were corrected for it was seen that the best signal was achieved when the sample was cold (Fig. S1), followed by when it was at room temperature, and finally a generally weaker signal intensity was observed when the system was warm. At warmer temperatures the field strength of the sensor would decrease, as seen in Fig. 3. Field strength is known to have a square dependence with respect to the signal intensity collected [30] so at higher temperatures the signal intensity would be lower.

It was shown that for each temperature there was a frequency where the signal intensity was optimal. This frequency did not correspond directly to the Larmor frequency at the center of the coil as shown in Fig. 3, with the optimal frequencies observed in Fig. 5 being higher. This was to be expected as the center of the coil was the point furthest from the either of the magnets, leading to the field strength at the center being lower than the surrounding volume. The RF probe was only able to excite a certain range of frequencies (which was dependent on the transmission bandwidth) so as the frequency was changed less of the sample could be successfully excited and therefore detected.

The achievable signal intensity substantially improved with different frequency settings. However, over the range of temperatures of interest the optimal frequency range was only 10.5 MHz to 11.0 MHz. If a frequency at the center of this range was to be selected (10.7 to 10.8 MHz) then a signal intensity close to the intensity at the optimal frequency would still be achievable. Therefore the idea of retuning the probe based on the temperature was seen to be unnecessary. Given the long term nature of clogging it would also be possible to only take T_1 measurements from a wetland during the months where the temperature was such that favorable signal intensity was achievable, however this might not be desirable or viable for certain applications.

A short study was conducted to try and localize the position of the regions within the RF coil that were not contributing signal. An 1.15 ± 0.05 mm ID capillary tube (Hawksley, Lancing, UK) was filled with water and magnetic resonance measurements were taken with it at different locations in the coil at room temperature (20 ± 0 °C), and while the system was both warm (52 ± 1 °C) and cool (9 ± 1 °C). For these experiments, additional averages were run in order to allow for a favorable signal to noise ratio (SNR). The tube, which ran the length of the coil in the z-axis, was placed at the extremes of the coil edge (top, bottom, far left, far right), and also moved through the entire height in the x-axis in 2 mm increments. Ultimately no significant change in the signal intensity was observed, suggesting that the sensitive region was fairly well distributed throughout the coil region. It was impractical to perform these experiments with a smaller sample tube.

3.3. Relaxation measurements as a function of temperature

It was of the most interest to confirm that the probe would provide representative T_1 relaxation data at different temperatures of operation, as the T_1 relaxation time would be used to monitor the wetlands clog state. Four T_1 measurements were taken at five different temperatures, where the probe was submerged into the water sample as before, and are shown on Fig. 6. Also presented on Fig. 6 are literature values of Simpson and Carr [17] from their comprehensive study of T_1 as a function of temperature for oxygen-free water between 0 and 50 °C.

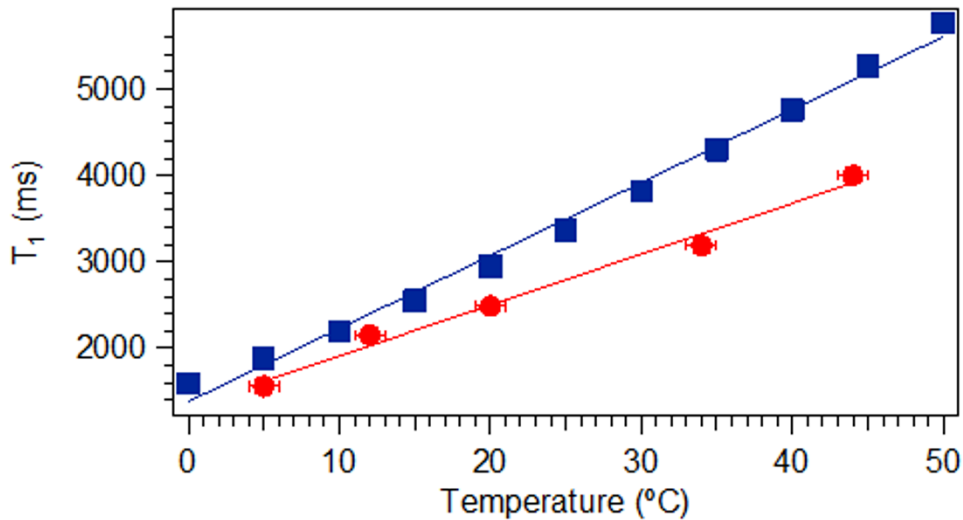


Fig. 6. T_1 relaxation of water with both the sensor and the sample held at five different temperatures ●. Values from work by Simpson and Carr's study on oxygen-free water [15] have been plotted between 0 and 50 °C ■.

For data taken using the sensor presented in this work, the linear fitting had a gradient of 58.9 ± 3.8 ms/°C and an intercept of 1320 ± 100 ms. Fitting the values reported by Simpson and Carr gave a gradient of 84.6 ± 2.3 ms/°C and an intercept of 1380 ± 70 ms.

It was clear that the general trend was the same, and that the intercept for both datasets were within the error of one another, with the gradient being slightly different. There were a number of potential reasons for the discrepancy in the gradient, the use of oxygenated water being the most likely candidate. As highlighted by Krynicky [18], earlier work often disregarded the important role that dissolved oxygen (which is highly paramagnetic) might cause on the relaxation values.

Comparing these results to ones where non-deoxygenated water was used [16], good agreement between the value at room temperature of 2.49 ± 0.01 s and their value of 2.3 s was seen. Ultimately, this agreement between data collected by the 'Helmholtz style' probe and literature values showed that the T_1 values collected at different temperatures were consistent.

Further to this, the validity of T_1 measurements in an actual wetland were investigated. Measurements were taken from a bed with insignificant levels of clogging over the course of 203 days, giving a temperature range from 7 – 16 °C. T_1 as a function of time has been plotted in Fig. 7(a), and against temperature in Fig. 7(b).

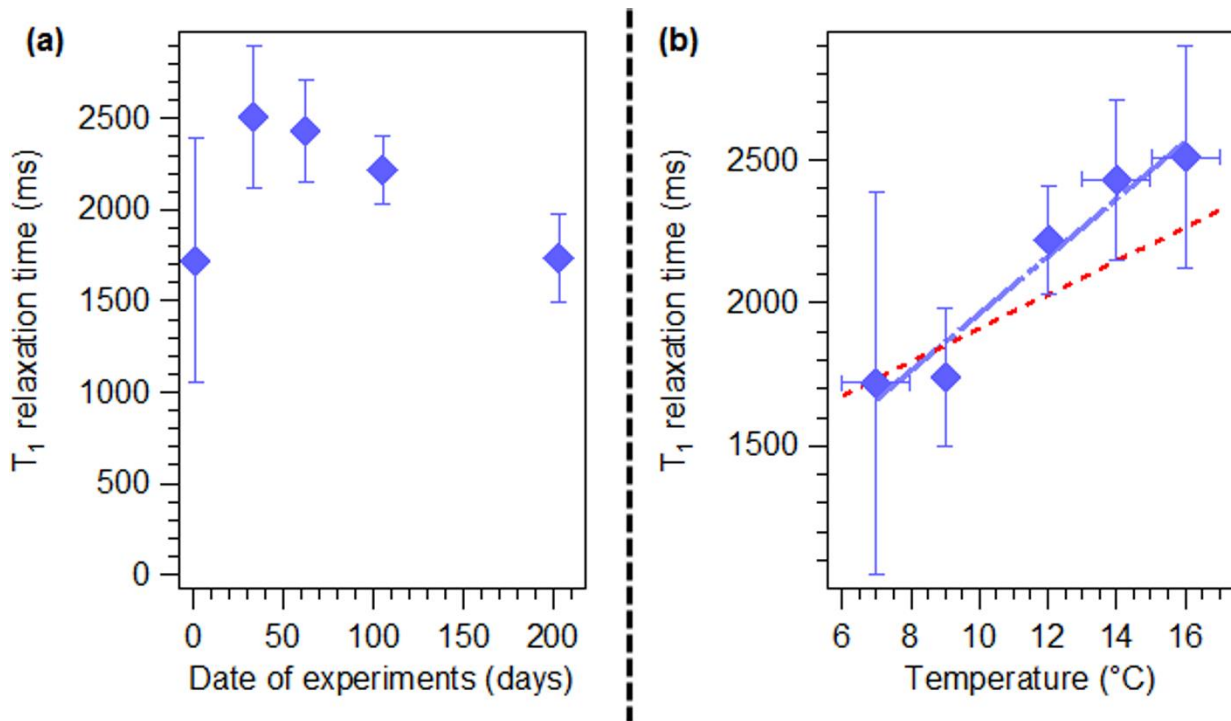


Fig. 7. T_1 relaxation recorded from a sensor embedded in an operational vertical flow wetland. Errors were extracted from the error in the mono-exponential fitting of the data. (a) T_1 relaxation measurements as a function of time. (b) T_1 relaxation measurements as a function of temperature. — shows the fitting of the T_1 values in the wetland against temperature, - - - shows the fitting of T_1 against temperature for water in the laboratory as previously shown in Fig. 6.

A functional relationship between the T_1 relaxation time and the date of the experiment was not apparent from Fig. 7(a), implying that significant clogging did not occur over this time scale (as would be expected, as clogging is a very long-term effect). Fig. 7(b) shows a strong linear relationship between the T_1 relaxation time and temperature with a gradient of 100.15 ± 13.5 ms/°C. This value was in agreement with the literature for water [17] within the error. It was further worth noting that the data only showed mono-exponential behaviour. It had previously been seen that the presence of water with significant concentrations of particulate in it, or water that makes up biofilm, would provide bi-exponential and tri-exponential components [13]. A single exponential suggested only the presence of free water, which supported the above result. It was therefore very unlikely that clogging had any notable influence on the recorded T_1 relaxation times, making the changes seen in Fig. 7 exclusively due to temperature.

The intercept of the fitting was lower than for the free-water datasets at 962 ± 162 ms. There were two likely reasons for this. The first reason was that the data in Fig. 7(b) covered a far smaller temperature range (7 to 16 °C) compared to the data in Fig. 6 (5 to 44 °C for the data collected on a comparable sensor), additionally the T_1 values had significantly larger errors. One factor that may have contributed to the larger T_1 errors *in situ* was the flow of water through the wetland, however this was very slow. It has been previously observed in the laboratory, using a model wetland system, that a slow flow has a minor effect on the SNR, and negligible effect on the value of T_1 .

Both the shorter temperature range and higher T_1 errors may have led to a slightly inaccurate fitting, where the fitting errors were smaller than what was representative. This was supported by plotting the data fitting collected in the laboratory onto the graph. The fitting

from the laboratory data (shown in red in Fig. 7(b)) went through all of the data points within their errors.

Further to this, it was conceivable that a very small amount of water with particulate existed in the part of the bed examined, but not a sufficient enough amount to be separately extracted in the fitting of the data. This may have reduced the overall T_1 values collected, creating an offset on the intercept. Previous work showed that the quantity of solid material within the wetland sample reduced the T_1 relaxation time [13], [14].

4. Conclusions

The aim of this work was to validate the ability to operate a permanent magnet MR clog state sensor design over a wide range of temperatures, covering the maximum likely scope that a constructed wetland deployed in Europe would experience. It was shown that this sensor was still able to collect MR measurements at high and low temperatures, confirming its suitability for long-term use in a wetland system.

An investigation was conducted into the signal losses at non-optimal frequencies at different temperatures; the optimal frequency being when the greatest signal intensity was achieved. Signal losses were incurred due to the limited bandwidth of the probe and the large magnetic field gradient within the volume of the solenoid. Different optimal frequencies were observed at different temperatures, as would be expected by the theory. Signal was seen to drop when the system was tuned to a non-optimal frequency, with reductions increasing as the frequency got further away from the ideal.

The validity of T_1 measurements at various temperatures have been shown with a water sample, with the recorded values agreeing with the literature. Further to this, measurements taken in an operational wetland were recorded over the course of 203 days. The data collected was in agreement with literature as well as with the laboratory results.

Acknowledgments

The research leading to these results has received funding from the European Union's Seventh Framework Programme managed by the REA – Research Executive Agency <http://ec.europa.eu/research/rea> (FP7/2007_2013) under project reference 606326. The work has been supported by the following partners: ARM Ltd. (UK), Lab-Tools Ltd. (UK), OxyGuard International A/S (Denmark), TechnoSAM SRL (Romania), Universitat Politècnica de Catalunya (Spain).

References

- [1] Liu, D., Ge, Y., Chang, J., Peng, C., Gu, B., Chan, G. Y., Wu, X.
Constructed wetlands in China: recent developments and future challenges.
Frontiers in Ecology and the Environment, 7 (2008), pp. 261-268
- [2] Zhang, D., Gersberg, R. M., Keat, T. S.
Constructed wetlands in China.
Ecological Engineering, 35(2009), pp. 1367-1378
- [3] Griffin, P., Wilson, L., Cooper, D.
Changes in the use, operation and design of sub-surface flow constructed wetlands in a major UK water utility.

Proceedings of the 11th International Conference on Wetland Systems for Water Pollution Control, Indore (2008)

[4] Morris, R. H., Knowles, P.

Measurement Techniques for Wastewater Filtration Systems.

In: Waste Water - Treatment and Reutilization, INTECH Open Access Publisher, (2011)

[5] Lin, A. Y. C., Debroux, J. F., Cunningham, J. A., Reinhard, M.

Comparison of rhodamine WT and bromide in the determination of hydraulic characteristics of constructed wetlands.

Ecological Engineering, 20 (2003), pp. 75-88

[6] Knowles, P. R., Griffin, P., Davies, P. A.

Complementary methods to investigate the development of clogging within a horizontal sub-surface flow tertiary treatment wetland.

Water research, 44 (2010), pp.320-330

[7] Tanner, C. C., Sukias, J. P., Upsdell, M. P.

Organic matter accumulation during maturation of gravel-bed constructed wetlands treating farm dairy wastewaters

Water Research, 32 (1998), pp. 3046-3054

[8] Nivala, J., Knowles, P., Dotro, G., García, J., Wallace, S.

Clogging in subsurface-flow treatment wetlands: measurement, modeling and management.

Water Research, 46 (2012), pp. 1625-1640

[9] Cano-Barrita, P.F.J., Marble, A. E., Balcom, B. J., García, J.C., Masthikin, I.V., Thomas, M.D.A., Bremner, T.W.

Embedded NMR sensors to monitor evaporable water loss caused by hydration and drying in Portland cement mortar.

Cement and Concrete Research, 39 (2009), pp. 324-328

[10] Morris, R. H., Newton, M. I., Knowles, P. R., Bencsik, M., Davies, P. A., Griffin, P., McHale, G.

Analysis of clogging in constructed wetlands using magnetic resonance.

Analyst, 136 (2011), pp. 2283-2286

[11] Bencsik, M., Shamim, M.F., Morris, R.H., Newton, M.I.

Monitoring accelerated clogging of a model horizontal sub-surface flow constructed wetland using magnetic resonance transverse relaxation times.

International Journal of Environmental Science and Technology, 178 (2013), pp. 48-52

[12] Shamim, M.F., Bencsik, M., Morris, R.H., Newton, M.I.

MRI measurements of dynamic clogging in porous systems using sterilised sludge.

Microporous and Mesoporous Materials, 178 (2013), 48-52.

[13] Hughes-Riley, T., Newton, M.I., Webber, J.B.W., Puigagut, J., Uggetti, E., Garcia, J., Morris, R.H.

Advances in Automated Reed Bed Installations.

2nd International Conference "Water resources and wetlands", Tulcea (2014)

[14] Hughes-Riley, T., Newton, M.I., Webber, J.B.W., Puigagut, J., Uggetti, E., Garcia, J., Morris, R.H.

Advances in clog state monitoring for use in automated reed bed installations.
Lakes reservoirs and ponds, 8 (2014), 52-65.

[15] Kadlec, R.H., Reddy, K. R.

Temperature Effects in Treatment Wetlands.

Water Environment Research, 73 (2001), pp. 543-557

[16] Bloembergen, N., Purcell, E. M., Pound, R. V.

Relaxation effects in nuclear magnetic resonance absorption.

Physical Review, 73 (1948), pp. 679

[17] Simpson, J. H., Carr, H. Y.

Diffusion and nuclear spin relaxation in water.

Physical Review, 111 (1958), pp. 1201

[18] Krynicky, K.

Proton spin-lattice relaxation in pure water between 0 C and 100 C.

Physica, 32 (1966), pp. 167-178

[19] Le Bihan, D., Delannoy, J., Levin, R. L.

Temperature mapping with MR imaging of molecular diffusion: application to hyperthermia.

Radiology, 171 (1989), pp. 853-857

[20] Cline, H. E., Hynynen, K., Hardy, C. J., Watkins, R. D., Schenck, J. F., Jolesz, F. A.

MR temperature mapping of focused ultrasound surgery.

Magnetic Resonance in Medicine, 31 (1994), pp. 628-636

[21] Bertsch, F., Mattner, J., Stehling, M. K., Müller-Lisse, U., Peller, M., Loeffler, R., Weber, J., Meßmer, K., Wilmanns, W., Issels, R., Reiser, M.

Non-invasive temperature mapping using MRI: comparison of two methods based on chemical shift and T1-relaxation.

Magnetic resonance imaging, 16 (1998), pp. 393-403

[22] Clegg, A. G., Coulson, I. M., Hilton, G., Wong, H.Y.

The temperature stability of NdFeB and NdFeBCo magnets.

IEEE Transactions on Magnetics, 26 (1991), pp. 1942-1944

[23] Hughes-Riley, T., Newton, M.I., Morris, R.H.

Temperature dependence of magnetic resonance sensors for embedding into constructed wetlands.

1st International Electronic Conference on Sensors and Applications, (2014)

[24] Hahn, E. L.

Spin echoes.

Physical review, 80 (1950), pp. 580

[25] Demas, V., Prado, P. J.

Compact magnets for magnetic resonance.

Concepts in Magnetic Resonance Part A, 34 (2009), pp. 48-59

[26] Fukushima, E., Roeder, S.B.W.
Experimental pulse NMR: A nuts and bolts approach.
Addison-Wesley, Reading (1981)

[27] Meiboom, S., Gill, D.
Modified spin-echo method for measuring nuclear relaxation times.
Review of scientific instruments, 29 (1958), pp. 688-691

[28] Hürlimann, M.D.
Diffusion and relaxation effects in general stray field NMR experiments.
Journal of Magnetic Resonance, 148 (2001), pp. 367-378

[29] Goelman, G., Prammer, M.G.
The CPMG pulse sequence in strong magnetic field gradients with applications to oil-well logging.
Journal of Magnetic Resonance, 113 (1995), pp. 11-18

[30] Hoult, D.I., Richards, R.
The signal-to-noise ratio of the nuclear magnetic resonance experiment.
Journal of Magnetic Resonance, 24 (1969), pp. 71-85

Supplementary materials for ‘Temperature dependence of magnetic resonance probes for use as embedded sensors in constructed wetlands’

Supplementary materials contains two additional graphs relating to the acquired signal intensity of the magnetic resonance sensor. Fig. S1 shows the signal intensity for the probe submerged in water at three different temperatures, after the data had been corrected for a discrepancy in the matching of the radio frequency transmit-receive electronics. This is an intermittent step between Fig. 5(a) and Fig. 5(b).

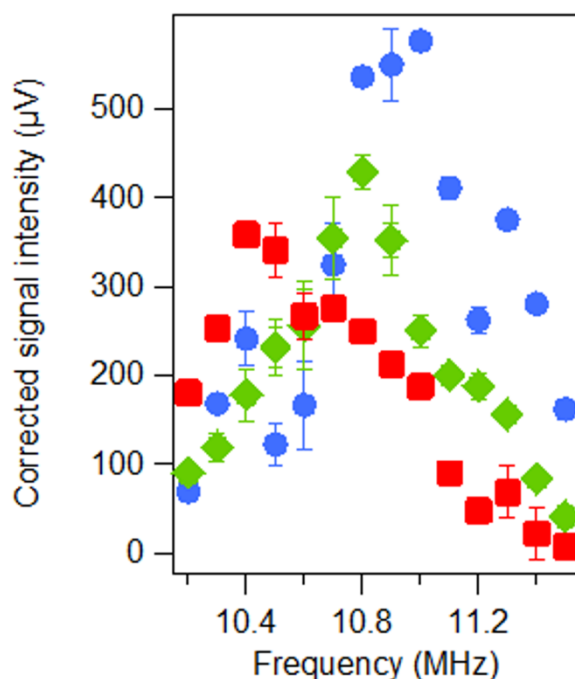


Fig. S1. Signal intensity as a function of frequency on a water sample with the sensor and sample held at three different temperatures: ● $2 \pm 0^\circ\text{C}$ ◆ $18 \pm 1^\circ\text{C}$ ■ $46 \pm 1^\circ\text{C}$. The collected signal intensity has been corrected to account for the discrepancy in the resonant circuits matching.

As highlighted in the experimental section, pulse lengths ranging from 3.8 μs to 8.1 μs were used depending on the resonant frequency, with longer pulse lengths typically being used for lower frequencies. The bandwidth was plotted as a function of the frequency (Fig. S2). This has been used to correct the data in Fig. 5(b) to also account for the fact that at certain frequencies different volumes of the sample would be detectable.

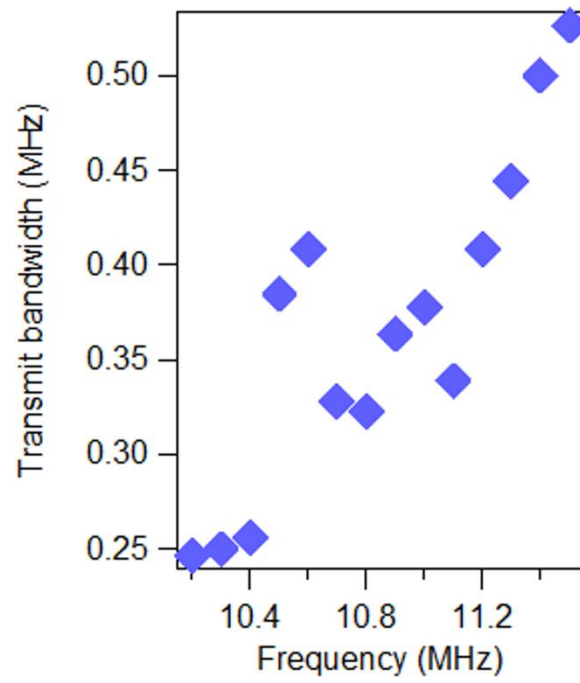


Fig. S2. The transmission bandwidth of the RF coil at different frequencies depending on the frequency being examined.